②

ARMY RESEARCH LABORATORY

ARL

Three-Dimensional Simulations of Normal Impact of Projectiles on Moving Targets

Anand Prakash

ARL-TR-326   December 1993

This document contains color plates: All DTIC reproductions will be in black and white

DTIC
SELECTE
FEB 24 1994
S B D

APPROVED FOR PUBLIC RELEASE; DISTRIBUTION IS UNLIMITED.

94 2 23   006

DTIC QUALITY INSPECTED 1

NOTICES

Destroy this report when it is no longer needed. DO NOT return it to the originator.

Additional copies of this report may be obtained from the National Technical Information Service, U.S. Department of Commerce, 5285 Port Royal Road, Springfield, VA 22161.

The findings of this report are not to be construed as an official Department of the Army position, unless so designated by other authorized documents.

The use of trade names or manufacturers' names in this report does not constitute indorsement of any commercial product.

REPORT DOCUMENTATION PAGE

Public reporting burden for this collection of information is estimated to average 1 hour per response, including the time for reviewing instructions, searching existing data sources, gathering and maintaining the data needed, and completing and reviewing the collection of information. Send comments regarding this burden estimate or any other aspect of this collection of information, including suggestions for reducing this burden, to Washington Headquarters Services, Directorate for Information Operations and Reports, 1215 Jefferson Davis Highway, Suite 1204, Arlington, VA 22202-4302, and to the Office of Management and Budget, Paperwork Reduction Project (0704-0188), Washington, DC 20503.

1. AGENCY USE ONLY (Leave blank)	2. REPORT DATE December 1993	3. REPORT TYPE AND DATES COVERED Final, Jan 91 - May 93

4. TITLE AND SUBTITLE

Three-Dimensional Simulations of Normal Impact of Projectiles on Moving Targets

5. FUNDING NUMBERS

PR: 1L162618AH80

6. AUTHOR(S)

Anand Prakash

7. PERFORMING ORGANIZATION NAME(S) AND ADDRESS(ES)

U.S. Army Research Laboratory
ATTN: AMSRL-WT-WD
Aberdeen Proving Ground, MD 21005-5066

8. PERFORMING ORGANIZATION REPORT NUMBER

9. SPONSORING / MONITORING AGENCY NAME(S) AND ADDRESS(ES)

U.S. Army Research Laboratory
ATTN: AMSRL-OP-CI-B (Tech Lib)
Aberdeen Proving Ground, MD 21005-5066

10. SPONSORING / MONITORING AGENCY REPORT NUMBER

ARL-TR-326

11. SUPPLEMENTARY NOTES

12a. DISTRIBUTION / AVAILABILITY STATEMENT

Approved for public release; distribution is unlimited.

12b. DISTRIBUTION CODE

13. ABSTRACT (Maximum 200 words)

Three-dimensional simulations of normal impact of 38.16-mm-long steel cylinders of L/D=6 on thin (1.59 mm) aluminum plates, which are themselves in motion, have been conducted using the HULL code on Cray supercomputers. HULL is an Eulerian code that uses a finite difference scheme to solve partial differential equations of continuum mechanics. An elastic-perfectly plastic model was used to describe the strain response of the target and the projectile. Simulations for projectile velocities of 219 m/s and 876 m/s, with the plates moving laterally ("edge-on") at 40 m/s and 160 m/s, respectively, are compared with cases when the plates are stationary. The transverse plate motion perpendicular to the projectile results in a time-dependent alteration of projectile motion and produces a tearing of the plate, in addition to the plugging that would occur if the plate were stationary. The results of the simulations are presented as graphic time histories of the physical quantities, including stress waves, in rod-plate interaction. These results show that if an armor plate is set in relative transverse motion with respect to an incidental projectile, it acquires a greater protection capability than the corresponding stationary plate. This has implications for armor applications, for live-fire testing, and for vulnerability and lethality analyses.

14. SUBJECT TERMS

impact; kinetic energy projectiles; rod-plate interaction; vulnerability; lethality; armor; computer simulation

15. NUMBER OF PAGES
25

16. PRICE CODE

17. SECURITY CLASSIFICATION OF REPORT UNCLASSIFIED	18. SECURITY CLASSIFICATION OF THIS PAGE UNCLASSIFIED	19. SECURITY CLASSIFICATION OF ABSTRACT UNCLASSIFIED	20. LIMITATION OF ABSTRACT SAR

INTENTIONALLY LEFT BLANK.

ACKNOWLEDGMENT

Accession For

NTIS GRA&I	☑
DTIC TAB	☐
Unannounced	☐
Justification	

By

Distribution/

Availability Codes

| Dist | Avail and/or Special |
| A-1 | |

INTENTIONALLY LEFT BLANK.

TABLE OF CONTENTS

INTENTIONALLY LEFT BLANK.

LIST OF FIGURES

INTENTIONALLY LEFT BLANK.

1. INTRODUCTION

One encounters the problem of impact of a projectile on a moving plate when a projectile is fired at a moving target from a stationary position or, equivalently, when a projectile is fired at a stationary target from a moving platform. Certain advanced protection concepts also involve interaction of moving plates with projectiles. A comprehensive series of computer simulations, which identified several protection schemes involving moving plates, was performed by the author during 1989-92 and has been reported elsewhere (e.g., Prakash 1992b). These simulations are not discussed here. The present report only addresses the general question of the effect of imparting a lateral velocity to a target plate on its protective capability against normally impacting cylindrical projectiles.

In normal impacts of blunt cylindrical projectiles on stationary thin plates, if the projectile velocity is high enough, the plate failure produces plugging. However, if the target plate is moving laterally (parallel to its plane), one expects the plugging to be accompanied by tearing of the plate due to its transverse motion perpendicular to the projectile. Moreover, the transfer of transverse momentum to the projectile would cause a deflection of the projectile, in addition to reducing its speed because of energy loss during the initial plug formation and the subsequent drag exerted by the moving plate. Depending upon the material properties, dimensions, and velocities involved, a host of phenomena (e.g., bending, dishing, heating, and erosion) would be exhibited by the projectile-plate system.

In attacking the problem theoretically, it is a complex task to model analytically all features of the projectile-plate interaction physics. One has two practical choices: build restricted and semi-empirical models or carry out a numerical simulation by advancing in small time steps solutions of the full equations of continuum physics. In the first approach, one concentrates on one aspect of the penetration problem by introducing simplifying assumptions (e.g., projectile rigidity), thus removing much of mathematical unpleasantness as well as some reality from the analytical process. The primary limitation of the second approach is that it requires fast computers with large memories. Although the selection of a computational mesh involves trade-offs between accuracy and economics, with the availability of modern supercomputers, large-scale problems of impact dynamics can be simulated realistically without resorting to the uncertainties of restricted modeling (Zukas & Kimsey 1990). The second approach was adopted in the present work. The Cray X-MP and Cray-2 supercomputers of the U. S. Army Research Laboratory were used to perform the simulations.

Three-dimensional (3-D) simulations of normal impact of 38.16-mm-long steel cylinders of 6.36-mm diameter, moving at 219 m/s, on a thin (1.59 mm) aluminum plate, which is

1

moving laterally (tangentially) with a velocity of 40 m/s, were carried out using the HULL code. (These impact parameters are identical to those of one of the recent experiments of Wu and Goldsmith [1990], but the projectile material used here is CR1010 steel, whereas tool steel was used in those experiments. Moreover, the experiments were conducted with the plate bolted down at the periphery, but the simulations here are for unconstrained, freely moving plates. The 3-D simulations presented here supersede the earlier 2-D simulations [Prakash 1991].) A second set of simulations was carried out in which both the projectile and plate velocities were increased by a factor of four, so that one has a projectile of velocity 876 m/s impacting a plate moving laterally at 160 m/s. These two sets of simulations were compared with simulations of two additional cases in which the plate is stationary but the projectile velocities are the same as in the first two cases. We focus our attention on how the projectile is affected as it perforates these plates. A partial summary of this work was reported elsewhere (Prakash 1992a).

2. THE SIMULATIONS

The simulations were performed with the HULL code (Matuska & Osborn 1986). HULL is an Eulerian code that uses a finite difference scheme to solve the partial differential equations of continuum mechanics. The hydrodynamic behavior of the metals is modeled using the Mie-Gruneisen equation of state. An elastic-perfectly plastic model was used to describe the strain response of the target and projectile, with a 2.0-kb yield strength for the (2024-0 Al) plate and 3.1-kb yield strength for the (cold-rolled SAE 1010 steel) projectile. These values were taken from Wu and Goldsmith (1990). Thermal softening parameters were included. The maximum principal strain model of material failure was used. When material failure occurs in a cell, a numerically significant void is introduced in the cell by replacing the material with air, which permits relaxation of the tensile forces, but recompression is permitted. Principal strain at failure was taken as 0.22 for the plate and 0.40 for the projectile. In all cases, the steel projectile was a 38.16-mm blunt cylinder of $L/D = 6$, and the thickness of the aluminum plate was 1.59 mm.

2.1 Case I. The Lower Velocity Impact. The initial configuration of the system at the beginning of the impact is shown in Figure 1. In the "laboratory" frame of reference, the initial plate velocity is 40 m/s to the left (i.e., in the negative x direction) and the projectile is moving vertically upward at 219 m/s. In the 3-D simulations, this initial direction of projectile velocity is taken as the positive z-axis (the positive and negative y-axis being the "fore" and "aft" directions). The problem has "fore"-"aft" planar symmetry so that the

3-D simulations can be done with only positive y values, with reflection symmetry about the x-z plane. However, there is no symmetry about the y-z plane for nonzero plate velocities. A 3-D Cartesian grid consisting of 120,064 cells, with a mesh size of 0.04 cm, was used. On Cray X-MP, the simulation took 9 min of CPU time for each microsecond of simulated (physical) time.
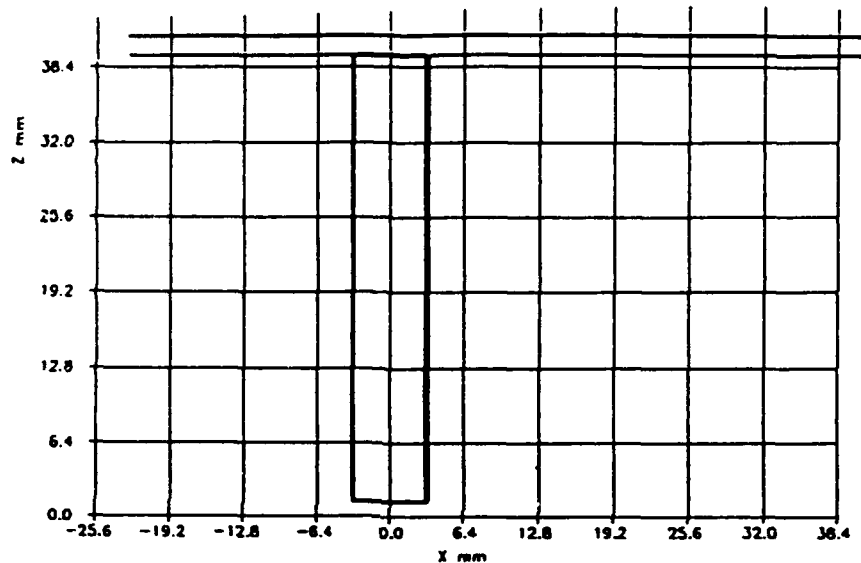

Figure 1. Projectile-plate system at 0 μs. (Computer mesh size is 0.4 mm.)

2.2 Case II. The Higher Velocity Impact. The problem, with the same geometry as above (see Figure 1), was simulated for a four-fold increase in both the projectile and the plate velocity. This simulation of normal impact of the cylindrical projectile of velocity 876 m/s on the 1.59-mm-thick aluminum plate, moving transversely at 160 m/s, was performed on a Cray-2 computer with a 3-D Cartesian grid consisting of 518,848 cells, with a mesh size of 0.0318 cm. It took 1 hr of CPU time to simulate each microsecond of physical time.

2.3 Cases III and IV. Impacts on Stationary Plate. Each of the previous two simulations was repeated with plate velocity set to zero. Thus, Case III consists of the cylindrical projectile moving in with a velocity of 219 m/s perpendicular to the stationary aluminum plate. In case IV, the cylindrical projectile impacts normally the stationary aluminum plate at a velocity of 876 m/s. These simulations were performed on the Cray-2.

3

3. RESULTS AND DISCUSSION

To study the evolution of the rod-plate interaction, density contours were plotted at an interval of several microseconds for Case I and Case II. Figure 2 shows the process of initial plugging at 25 μs after impact, for Case I, the lower projectile velocity impact. Figure 3 shows the situation at 100 μs after impact. To compare it with the higher velocity case, we note that in Case II, the projectile is crossing the plate at a rate which is about four times faster than in Case I. Thus, the 100-μs situation of Case I is to be compared with the state of affairs at 25 μs of Case II, shown in Figure 4. Such a comparison shows that the overall tilt of the projectile is larger in Case I, but the head of the (nonrigid steel) projectile is more distorted and bent (in the negative x direction) in Case II. For Case II, the rear end of the projectile passes through the plane of the plate at 45 μs, as shown in Figure 5.

In both cases, we find that after the initial plugging, the subsequent part of the penetration process exhibits a "tearing" of the plate due to the transverse motion of the plate relative to the projectile, a feature that does not occur if the plate is stationary. As shown in Figure 3 and Figure 4, the lengths of the corresponding slots formed in the plate after traversal of vertical (z) distance by the projectile in Case I and Case II are 0.8 cm and 1.06 cm, respectively. Since the plates would also travel an equal lateral distance during these times, one might have expected the slot lengths to be about the same in Figures 3 and 4. The observed difference is apparently because of the fact that in the higher velocity impact, part of the left rim of the crater in the plate was severed during the earlier stages of the impact. Clearly, we see that the rod-plate interaction is not velocity scalable in that a quadrupling of plate velocity does not compensate for a quadrupling of rod velocity, even in slot formation.

Figures 6 and 7 show, for Case I, the time histories of the vertical (z direction) velocity, w, and the transverse (x direction) velocity, u, of the projectile tip. Figures 8 and 9 display the same physical quantities for Case II. The impact of the moving plate with the cylindrical projectile produces longitudinal waves, transverse waves, and reflected waves at material boundaries. As a material property input, we used the longitudinal (sound) wave velocity in steel of 4.6 km/s. The wave transit time along the length of the projectile is approximately 8 μs. The oscillations in vertical velocity, shown in Figure 6, with a period of approximately 16 μs, are attributable to longitudinal waves induced in the projectile by the impact. The early time oscillations, seen in Figures 6 and 8, are produced during the process of plugging, largely due to multiple wave reflections in the thin plate. The duration of their appearance is roughly equal to the transit time of the rod through a distance equal to the plate thickness. The nominal transit time is 7.2 μs for Case I and 1.8 μs for Case II. The
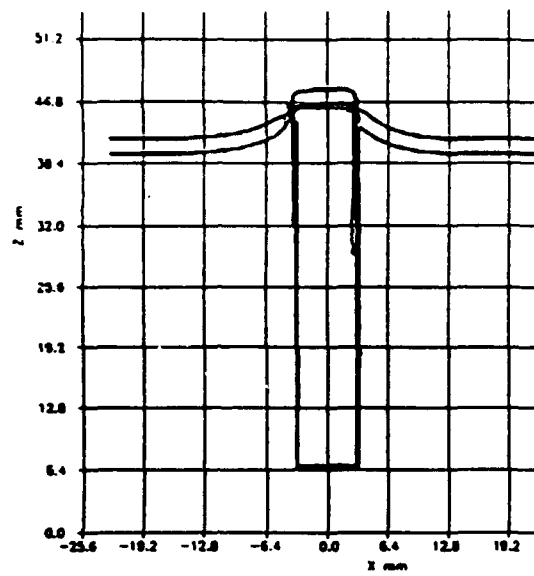
4

Figure 2. Case I at 25 μs after impact.

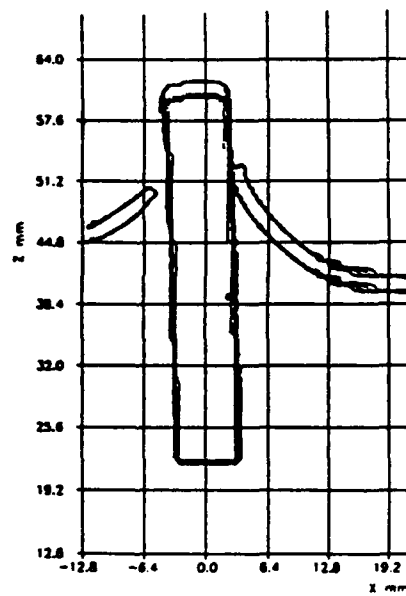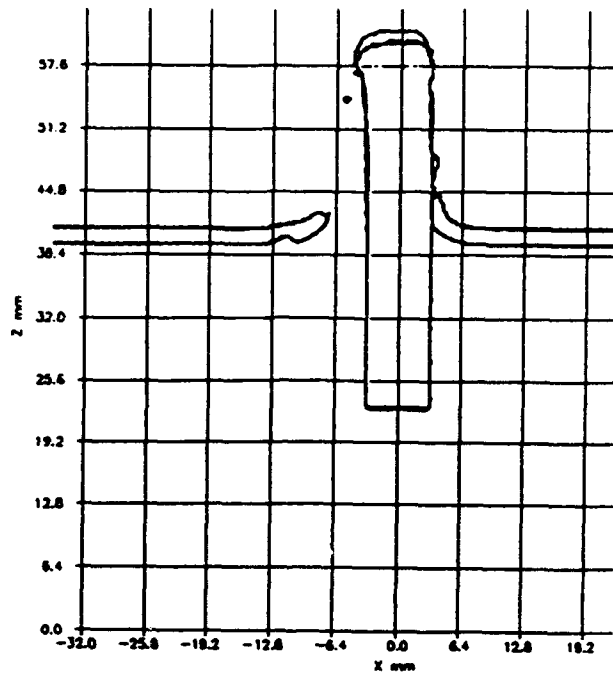**Figure 3.** Case I at 100 μs after impact.

5

Figure 4. Case II at 25 μs after impact.
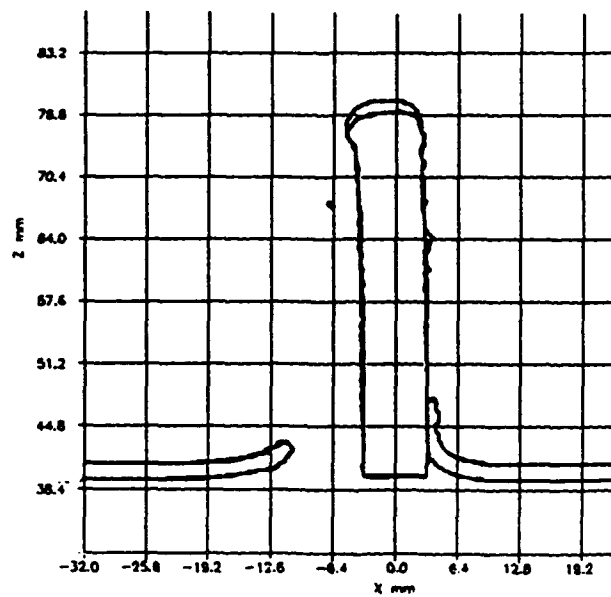

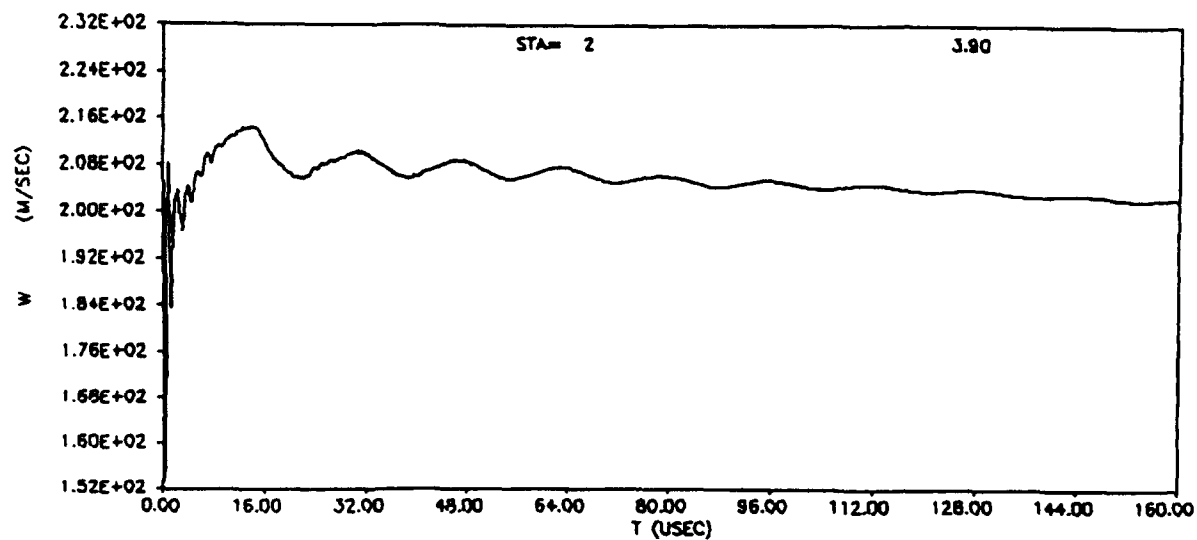**Figure 5.** Case II at 45 μs after impact.

6

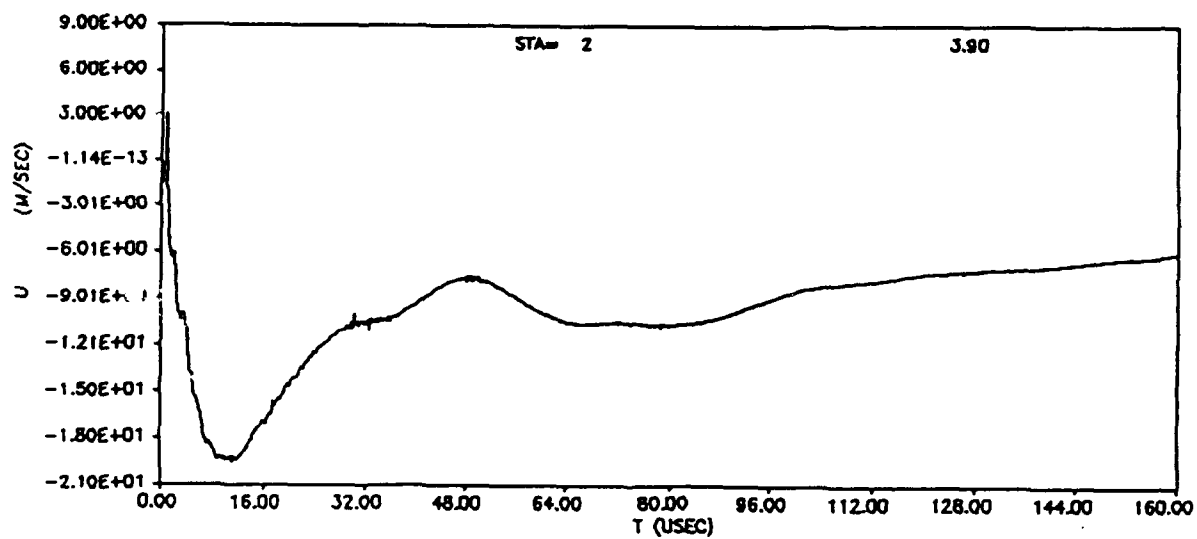Figure 6. Vertical projectile-tip velocity, Case I.

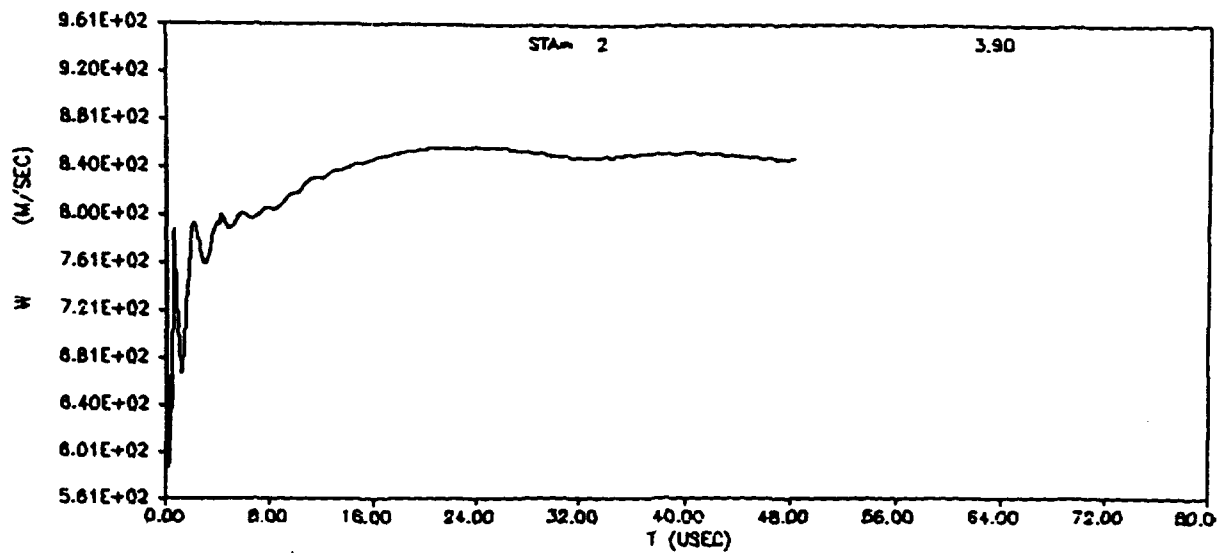Figure 7. Horizontal projectile-tip velocity, Case I.

7

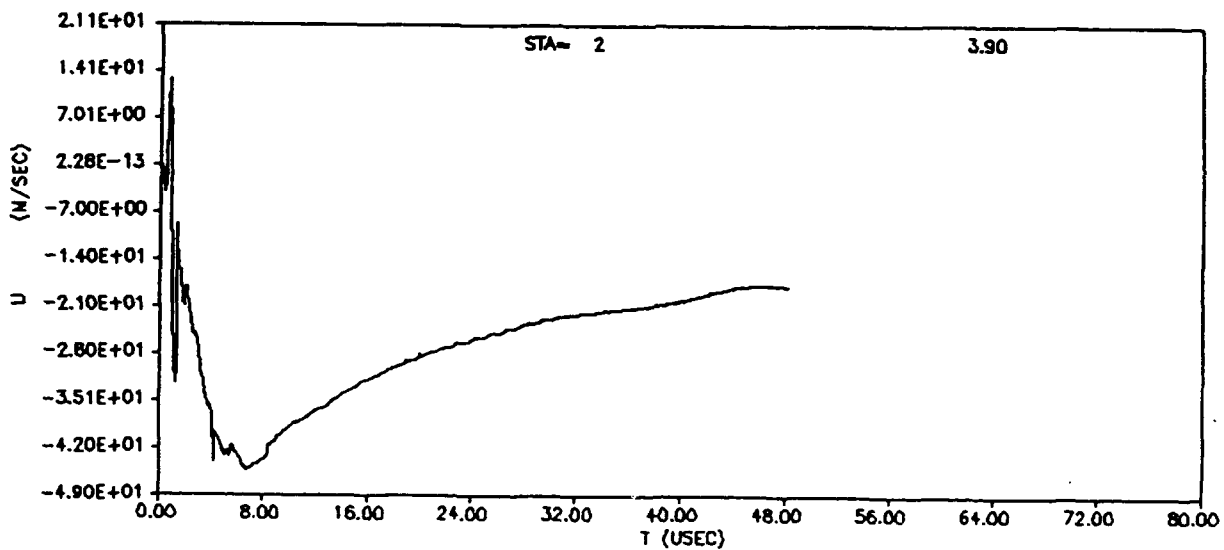**Figure 8.** Vertical projectile-tip velocity, Case II.

Figure 9. Horizontal projectile-tip velocity, Case II.

overall oscillations seen in Figures 6 and 8 are the net effect of several contributions. The compression transmitted to the plate by initial impact of the projectile is reflected as a rarefaction (tension) from the opposite face of the plate, and, on reaching the rod-plate interface, it is partially transmitted into the rod and partially reflected back into the plate because of impedance mismatch at the interface. Moreover, lateral (radial) rarefactions emanate from the free surface of the projectile, when the compression transmitted to the projectile by initial impact reaches its surface. The dispersive nature of some of the waves is a further complication. The resulting net oscillations of pressure in the rod, at a point near its tip, can be seen in the time history plots of pressure, shown in Figures 10 and 11.

The 3-D stress wave patterns generated in the projectile are quite complicated, especially because of dispersive oscillations and multiple reflections at material boundaries. Snapshots of the cross-sections of the time-dependent 3-D stress wave patterns, obtained from the HULL code simulations for Case II, at 3.8 μs, 5.0 μs, 8.8 μs, and 10 μs after impact, are shown in Figures 12, 13, 14, and 15, respectively. These are raster plots of pressure and are color coded so that green, yellow, and magenta represent positive pressures (compression) and blue, red, and grey represent negative pressures (tension). It would be difficult to obtain analytically these time-varying wave patterns in the rod. The formation of regions of high tensile stress at separate locations in the projectile is indicative of the possibility of projectile break-up into two or more segments, for some suitable rod-plate parameters. We also notice that the plate is under compression near the region of contact on the right-hand side, and it is under tension in the region to the left of the projectile. This is so because the plate is moving laterally from the right to the left.

We now examine the changes in rod velocity produced by its interaction with the moving target plates. For Case I, the vertical velocity (w) of the tip of the projectile at 100 μs is about 205 m/s, so that it has lost approximately 14 m/s of vertical velocity. However, it has acquired a horizontal velocity (u) because of momentum transfer from the moving plate. As shown in Figure 7, u = -9 m/s at 100 μs, and it decreases in magnitude to u = -5.6 m/s, at 160 μs. For the higher velocity case, Figure 8 shows that at 45 μs, when the projectile is finally exiting the plate, the vertical velocity, w, of the tip is approximately 847 m/s. Thus, it has lost 29 m/s of vertical velocity during the impact. Again, as shown in Figure 9, the projectile has acquired a horizontal velocity, u = -20 m/s because of momentum transfer from the moving plate. It may be noted that the Lagrangian station, which records the rod tip velocities, was taken in the rod material just inside the front end of the rod but slightly off-axis to the right (x =0.01 cm). In the initial stages of the impact, the radial distortion of the front end of the rod gives a positive velocity (u) to this station, as can be seen in Figures 7 and 9.

9

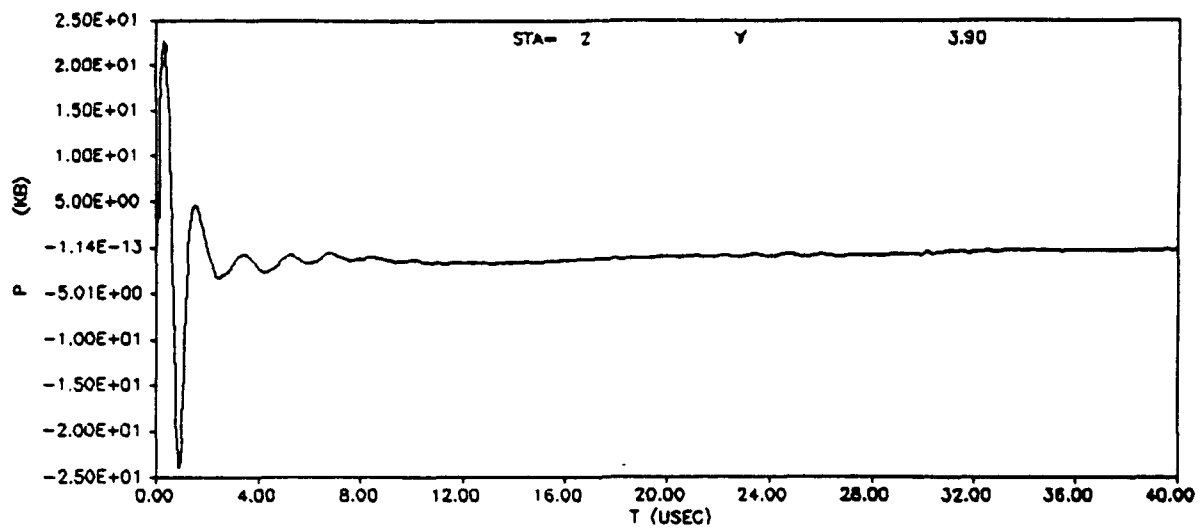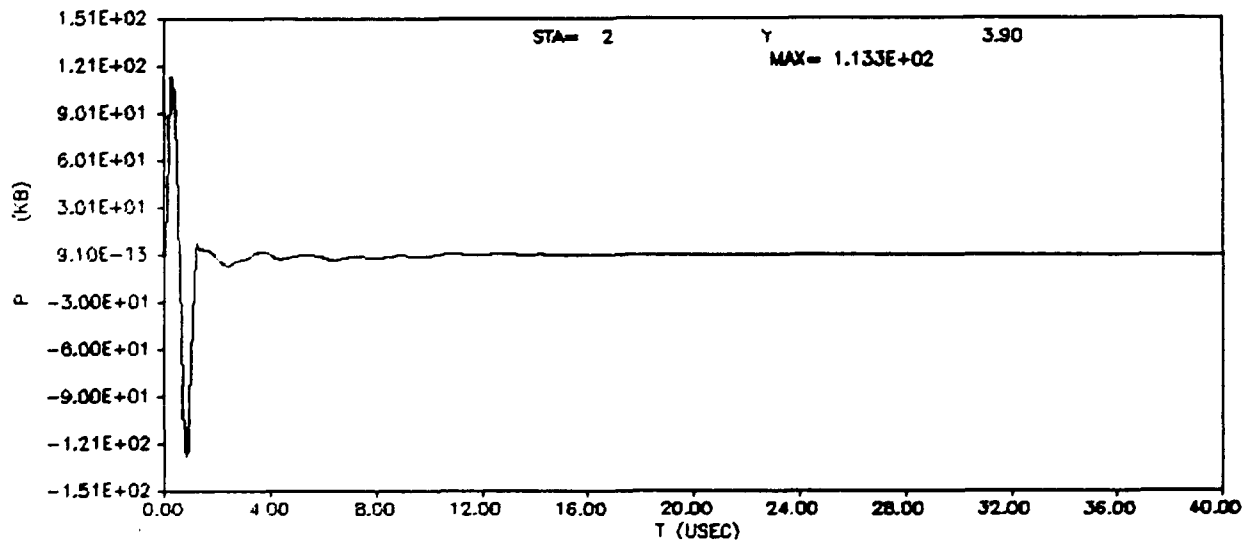**Figure 10.** Time history of pressure at rod tip for Case I.

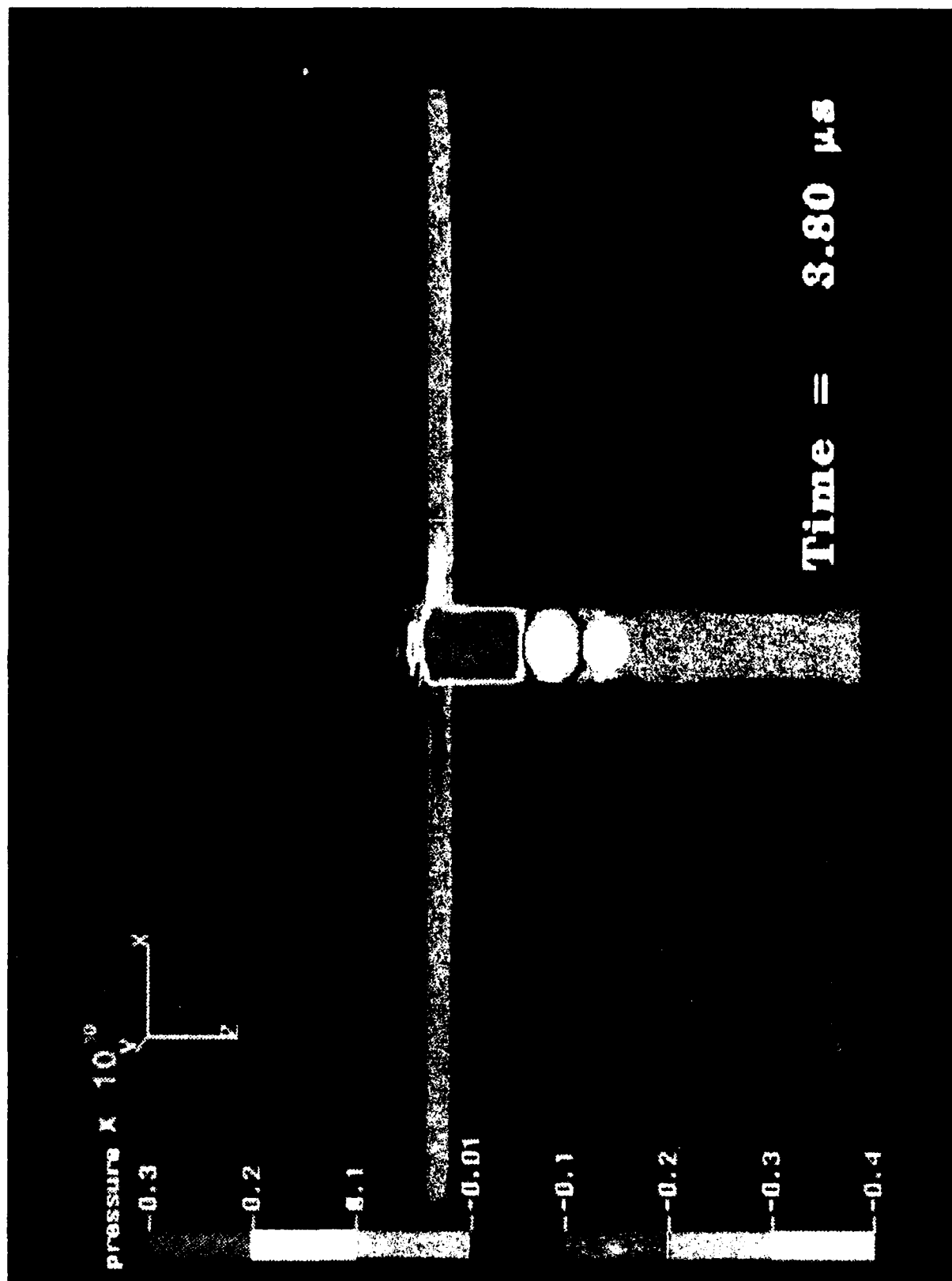**Figure 11.** Time history of pressure at rod tip for Case II.

10

Figure 12. Stress wave pattern 3.8 μs after impact.
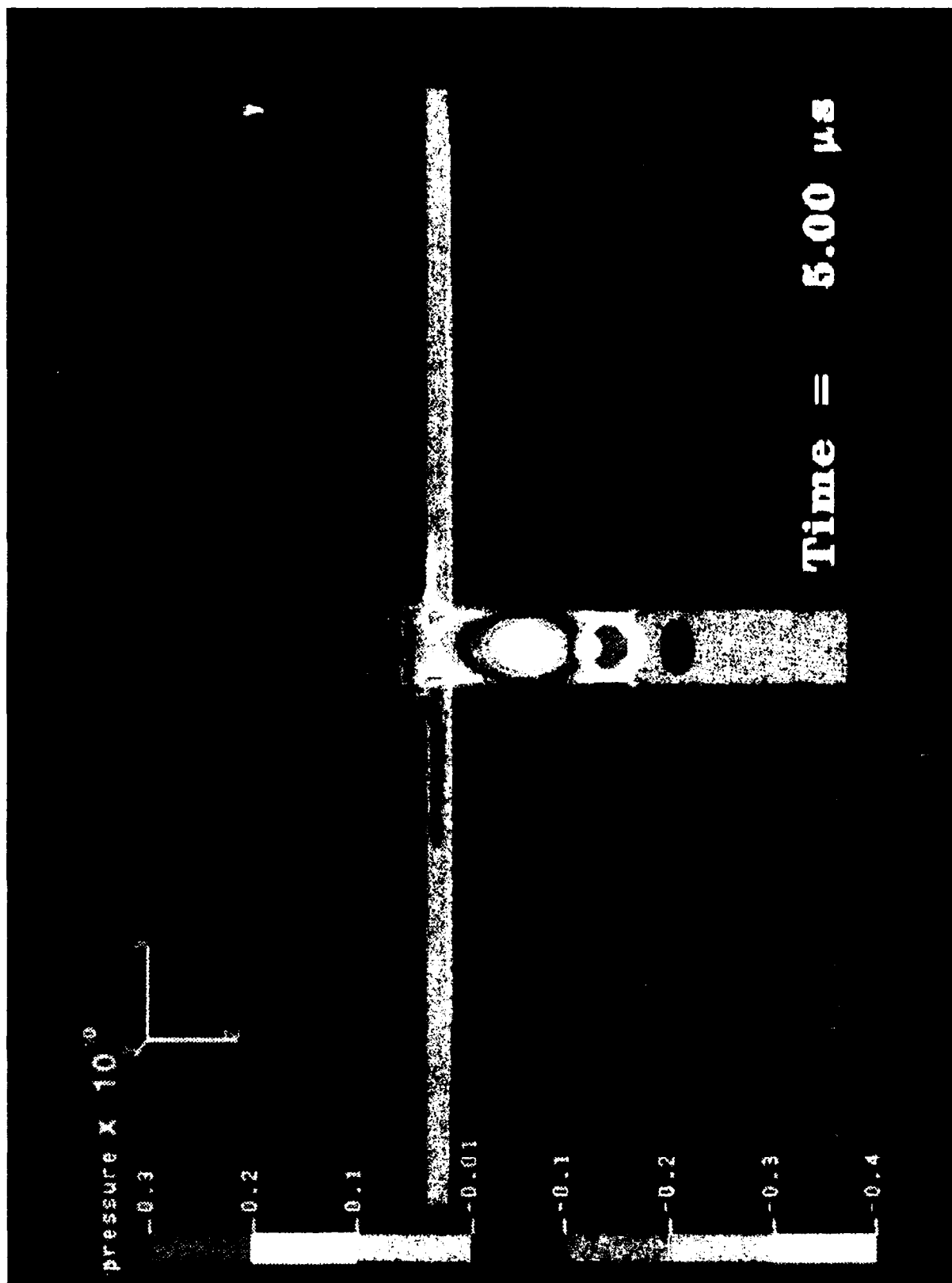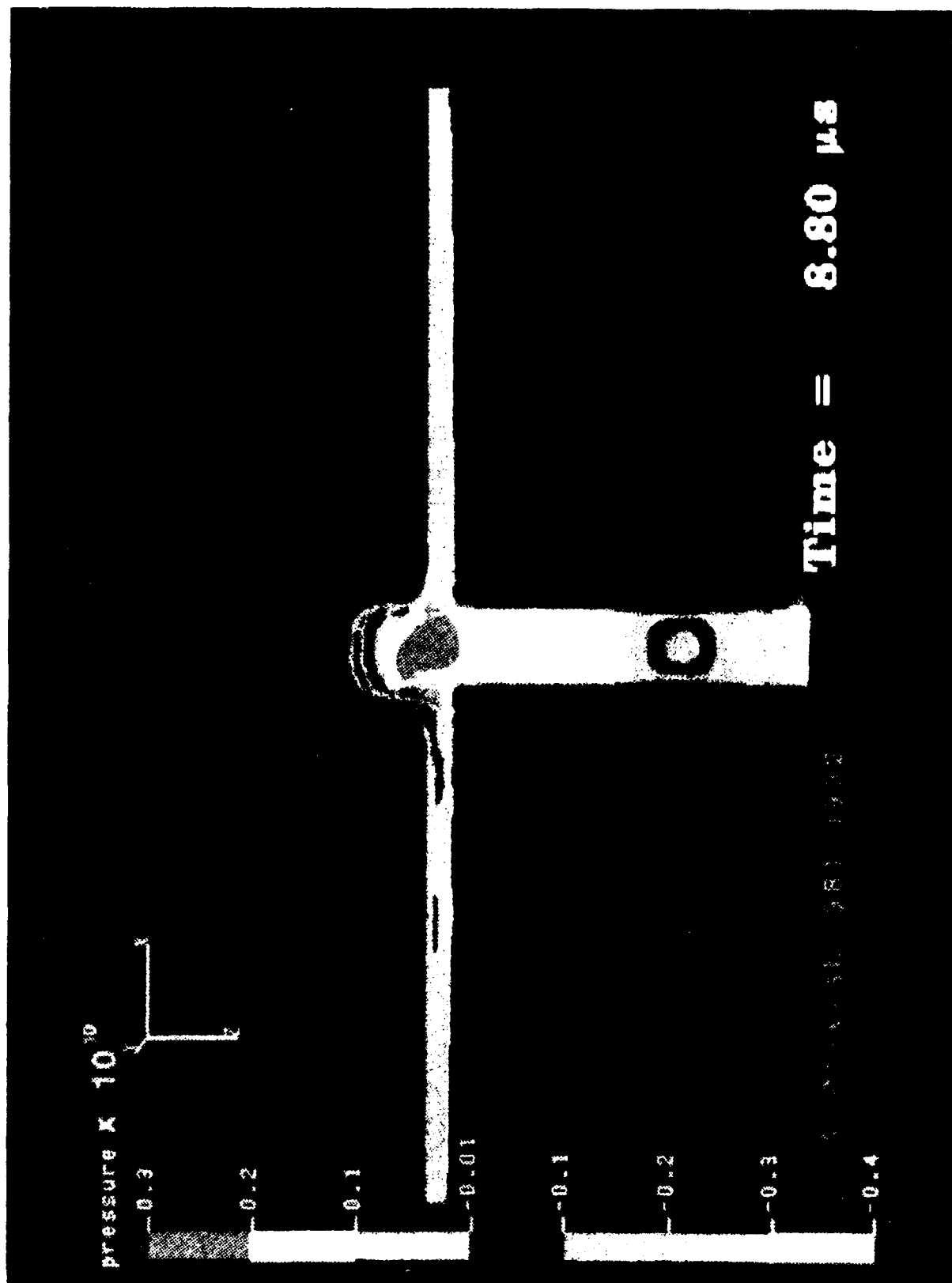
Figure 13. Stress wave pattern 5.0 µs after impact.
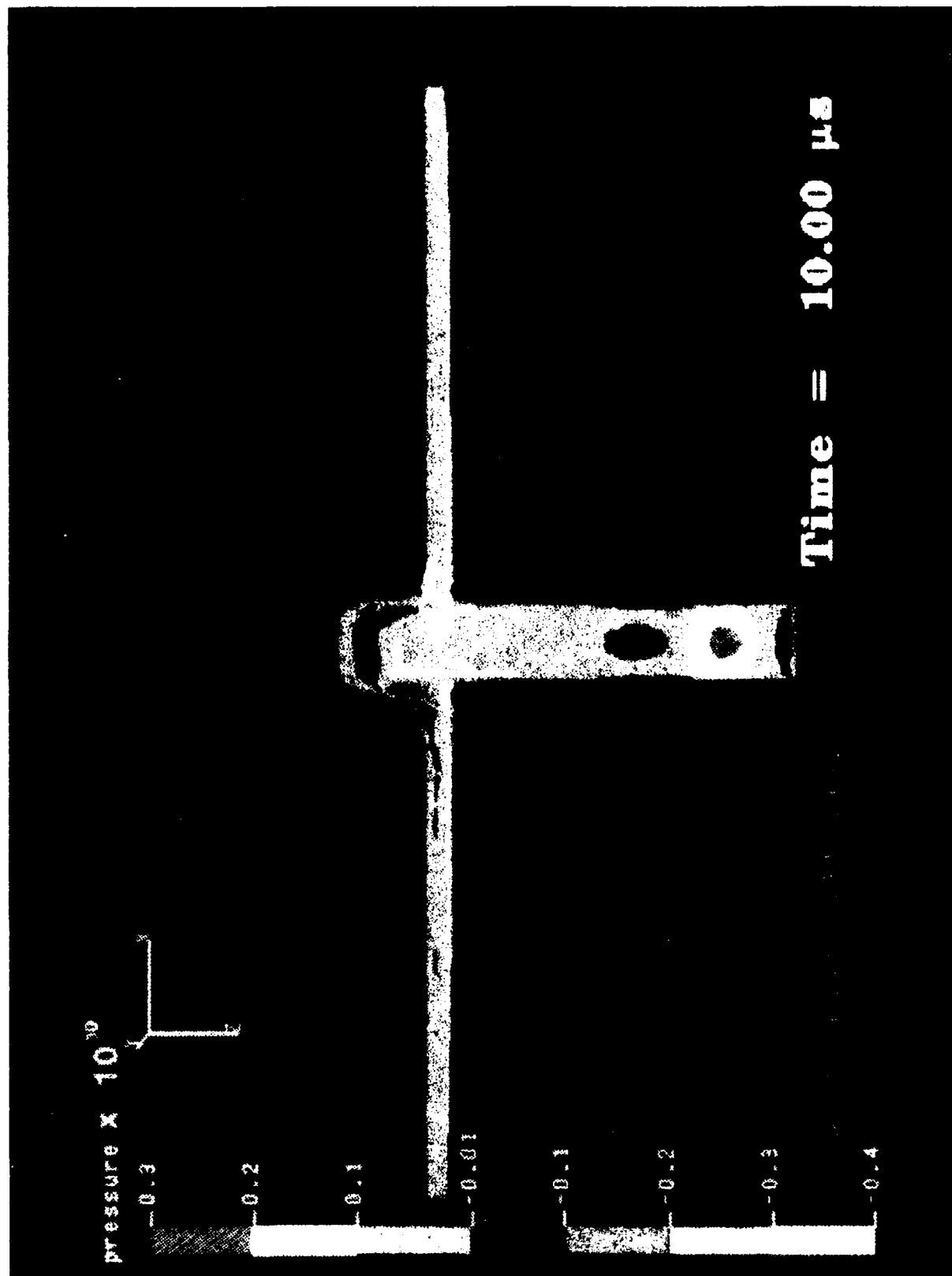
Figure 14. Stress wave pattern 8.8 μs after impact

Following page intentionally left blank.

Figure 15. Stress wave pattern 10 μs after impact.

Following page intentionally left blank.

We also find that the horizontal velocity (u) acquired is a function of position along the length of the projectile. At any given time, the horizontal velocity decreases in magnitude as one moves back from the tip of the projectile. Thus, in the low velocity case, for example, at 100 μs, when $u = -9$ m/s near the tip, one finds that $u = -3.2$ m/s at a Lagrangian station near the center of mass of the projectile. This variation is partly indicative of a counterclockwise rotational velocity. A time-dependent bending strain is also a contributing factor. It should also be noted that because of the dissipative interaction of the moving plate with the (right-hand) side of the cylindrical projectile, which continues until the tail-end of the projectile has cleared the plate, the vertical (axial) projectile velocity shows a general decrease in magnitude with time after plugging. Moreover, the tilt induced in the projectile, by the plate motion, keeps on changing until the projectile has cleared the plate.

Finally, we compare the moving plate cases, Cases I and II, with the corresponding static plate cases, Cases III and IV. We find that the time histories of vertical velocity (w) of the projectile tip in the 3-D simulations of Cases III and IV show similar large amplitude oscillations as in Cases I and II, but now there is no general decrease in the magnitude of the (average) vertical velocity with time after plugging. Also, the magnitude of loss of the vertical projectile velocity in traversing the plate is much smaller.

For the 219-m/s projectile velocity, with the plate stationary, we find that the loss of the vertical velocity (at 100 μs) is only 9.5 m/s, compared to the loss of 14 m/s when the plate had a lateral velocity of 40 m/s. For the higher velocity case, when the projectile strikes the stationary plate at 876 m/s, the loss of the vertical velocity in traversing the plate (at 45 μs) is just 19 m/s, as compared to 29 m/s for the moving plate ($u = 160$ m/s) case. Thus, an armor plate, in relative transverse motion with respect to an impacting projectile, acquires a greater protection capability merely by virtue of its motion. This result is consistent with the results of other recent studies which concentrated on ballistic limits (Wu & Goldsmith 1990) or shaped charges (Held 1992).

4. CONCLUSIONS AND RECOMMENDATIONS

The impact dynamics of cylindrical projectiles that strike perpendicularly on plates, which are themselves in lateral motion, was investigated by carrying out computer simulations of the rod-plate interaction with the HULL code. HULL is an Eulerian code that uses a finite difference scheme to solve the partial differential equations of continuum mechanics, with material properties as an input. An elastic-perfectly plastic model was used to describe the strain response of the target and the projectile. Three-dimensional simulations of normal impact of 38.16-mm-long steel cylinders, with $L/D = 6$, moving with initial velocities

19

of 219 m/s and 876 m/s, on thin (1.59 mm) aluminum plates, moving laterally (parallel to their face) at 0 m/s, 40 m/s and 160 m/s, were performed on Cray supercomputers. The stress wave patterns generated in the projectile-plate system are quite complicated, especially because of multiple reflections, in three dimensions, at the material boundaries. The simulations enabled us to produce color-coded quantitative visualizations of space-time variations of the stresses propagated in the system. Time histories of several physical quantities of interest were also plotted, and compared, for different initial values of rod-plate parameters.

For impact with initial projectile velocity of 219 m/s, we find that the velocity of the rod in the original direction is reduced by 14 m/s when the plate is moving with an initial lateral velocity of 40 m/s, as compared to a reduction of 9.5 m/s for the case of the stationary plate. When both the projectile velocity and the plate velocity are quadrupled, so that the cylindrical projectile moving at 876 m/s impacts perpendicular to the plate moving with initial lateral velocity of 160 m/s, the loss of projectile velocity in its original direction of motion is 29 m/s, as compared to a loss of 19 m/s for the stationary plate. Moreover, because of transfer of transverse momentum from the moving plate to the projectile, the rod undergoes deflection and rotation and suffers side erosion so that after perforation of the plate, it would have a lower residual penetration in a back-up passive armor than a rod that perforates the same plate in an initially stationary state. It was, however, seen that the rod-plate interaction is not velocity scalable in a simple manner in that a quadrupling of plate velocity together with a quadrupling of rod velocity did not leave the actual slot length invariant, for the velocities considered here.

It is concluded that if an armor plate is set in relative transverse motion with respect to an impacting cylindrical projectile, the plate acquires a greater protection capability than the same plate in an initially stationary state.

The results obtained have direct implications in two areas: use of moving plates for armor, and vulnerability and lethality measurements. A series of computer simulations of interactions of moving plates with rods was performed by the author during 1989-1992 for the purpose of identifying new protection schemes, and these simulations are the subject of other reports (e.g., Prakash 1992b). The implications in the area of vulnerability and lethality studies are discussed below.

This work has implications for vulnerability and lethality analyses for cases when a projectile is fired at a moving target (e.g., a helicopter) from a stationary position (e.g., an antiaircraft battery) or, equivalently, when a projectile is fired at a stationary target from a moving platform (e.g., air-to-ground attack). If the vulnerability and lethality analyses neglect the effect of relative transverse motion of the projectile and target surface, the results

20

would not be exactly what would happen in actual combat. This also applies to live-fire testing, if the vulnerability and lethality measurements involving helicopters or missiles are conducted at a test site with the firing platform and target kept stationary. The magnitude of the error is dependent on the magnitude of relative transverse velocity in actual combat.

Since, the use of moving targets or platforms in live-fire tests is burdensome, one might consider performing a series of full computer simulations, of the kind presented here, to derive some approximate algorithms for correcting the results of stationary live-fire tests to actual combat scenarios that involve relative transverse velocities. Similarly, modifications of the details of spall patterns, used in analytical studies of vulnerability and lethality, for scenarios involving moving targets or moving platforms, might be obtainable by performing a series of computer simulations of the kind described here.

INTENTIONALLY LEFT BLANK.

5. REFERENCES

Held, M. Private communication with the author. Stockholm, June 3, 1992.

Matuska, D. A., and J. J. Osborn. HULL Documentation. Orlando Technology Inc., Shalimar, Florida, 1986.

Prakash, A. "Supercomputer Simulations of Impact of Cylindrical Projectiles on Moving Plates." The Proceedings of 1991 Summer Computer Simulation Conference, edited by Dale Pace, published by The Society for Computer Simulation, San Diego, CA, pp. 543-547, 1991.

Prakash, A. "Three Dimensional Simulations of Impact of Projectiles on Moving Plates." Ballistics '92. 13th International Symposium, June 1-3, Stockholm, 1992, vol. 3, National Defense Research Establishment, Stockholm, Sweden, pp. 69-75, 1992a.

Prakash, A. "Simulations of Interaction Dynamics and Residual Penetration of KE Rods Impacting on Moving Plates." Proceedings of Second Ballistics Symposium on Classified Topics, held at Johns Hopkins University, Laurel, MD, October 26-29, 1992, published by American Defense Preparedness Association and Army Research Laboratory, pp. 183-192, 1992b.

Wu, E., and W. Goldsmith. "Normal Impact of Blunt Projectiles on Moving Targets: Experimental Study." International Journal of Impact Engineering, vol. 9, pp. 389-404, 1990.

Zukas, J. A., and K. D. Kimsey. "Supercomputing and Computational Penetration Mechanics." BRL-TR-3143, U. S. Army Ballistic Research Laboratory, Aberdeen Proving Ground, MD, 1990.

INTENTIONALLY LEFT BLANK.

No. of
Copies Organization

2   Administrator
    Defense Technical Info Center
    ATTN: DTIC-DDA
    Cameron Station
    Alexandria, VA 22304-6145

1   Commander
    U.S. Army Materiel Command
    ATTN: AMCAM
    5001 Eisenhower Ave.
    Alexandria, VA 22333-0001

1   Director
    U.S. Army Research Laboratory
    ATTN: AMSRL-OP-CI-AD,
            Tech Publishing
    2800 Powder Mill Rd.
    Adelphi, MD 20783-1145

1   Director
    U.S. Army Research Laboratory
    ATTN: AMSRL-OP-CI-AD,
            Records Management
    2800 Powder Mill Rd.
    Adelphi, MD 20783-1145

2   Commander
    U.S. Army Armament Research,
      Development, and Engineering Center
    ATTN: SMCAR-IMI-I
    Picatinny Arsenal, NJ 07806-5000

2   Commander
    U.S. Army Armament Research,
      Development, and Engineering Center
    ATTN: SMCAR-TDC
    Picatinny Arsenal, NJ 07806-5000

1   Director
    Benet Weapons Laboratory
    U.S. Army Armament Research,
      Development, and Engineering Center
    ATTN: SMCAR-CCB-TL
    Watervliet, NY 12189-4050

1   Director
    U.S. Army Advanced Systems Research
      and Analysis Office (ATCOM)
    ATTN: AMSAT-R-NR, M/S 219-1
    Ames Research Center
    Moffett Field, CA 94035-1000

No. of
Copies Organization

1   Commander
    U.S. Army Missile Command
    ATTN: AMSMI-RD-CS-R (DOC)
    Redstone Arsenal, AL 35898-5010

1   Commander
    U.S. Army Tank-Automotive Command
    ATTN: AMSTA-JSK (Armor Eng. Br.)
    Warren, MI 48397-5000

1   Director
    U.S. Army TRADOC Analysis Command
    ATTN: ATRC-WSR
    White Sands Missile Range, NM 88002-5502

(Class. only) 1   Commandant
    U.S. Army Infantry School
    ATTN: ATSH-CD (Security Mgr.)
    Fort Benning, GA 31905-5660

(Unclass. only) 1   Commandant
    U.S. Army Infantry School
    ATTN: ATSH-WCB-O
    Fort Benning, GA 31905-5000

1   WL/MNOI
    Eglin AFB, FL 32542-5000

Aberdeen Proving Ground

2   Dir, USAMSAA
    ATTN: AMXSY-D
            AMXSY-MP, H. Cohen

1   Cdr, USATECOM
    ATTN: AMSTE-TC

1   Dir, USAERDEC
    ATTN: SCBRD-RT

1   Cdr, USACBDCOM
    ATTN: AMSCB-CII

1   Dir, USARL
    ATTN: AMSRL-SL-I

5   Dir, USARL
    ATTN: AMSRL-OP-CI-B (Tech Lib)

No. of Copies	Organization	No. of Copies	Organization
1	Commander U.S. Army Strategic Defense Command ATTN: CSSD-H-LL, T. Crowles Huntsville, AL 35807-3801	1	Orlando Technology, Inc. ATTN: D. Matuska P.O. Box 855 Shalimar, FL 32579
1	Commander U.S. Army Military Academy Department of Mathematics ATTN: COL R. A. Kolb West Point, NY 10996-1786	1	Kaman Sciences Corporation ATTN: D. Barnette P.O. Box 7463 Colorado Springs, CO 80933
2	Commander USA TARDEC ATTN: AMCPM-ABMS-SA, J. Rowe AMSTA-RSS, K. D. Bishnoi Warren, MI 48397-5000	1	General Dynamics ATTN: J. H. Cuadros Mail Zone 601-87 P.O. Box 50-800 Ontario, CA 91761-1085
1	Director DARPA ATTN: J. Richardson 3701 North Fairfax Dr. Arlington, VA 22203-1714	1	E. I. DuPont De Nemours & Co. ATTN: B. Scott P.O. Box 1635 Wilmington, DE 19899
2	Air Force Armament Laboratory ATTN: AFATL/DLJW, W. Cook AFATL/MNW, LT D. Lorey Eglin AFB, FL 32542	1	SRI International ATTN: Dr. L. Seaman 333 Ravenswood Ave. Menlo Park, CA 94025
1	AFATL-DLJR ATTN: J. Foster Eglin AFB, FL 32542	1	Martin Marietta Aerospace ATTN: D. R. Bragg MP 109 P.O. Box 5837 Orlando, FL 32855
1	Rockwell International Rocketdyne Division ATTN: J. Moldenhauer, HB 23 6633 Canoga Ave. Canoga Park, CA 91303	1	Northrop Corporation Electro-Mechanical Division ATTN: D. L. Hall 500 E. Orangethorpe Ave. Anaheim, CA 92801
2	McDonnell Douglas Helicopter ATTN: MS 543-D216, L. R. Bird L. A. Mason 5000 E. McDowell Rd. Mesa, AZ 85205	1	Boeing Aerospace Company Shock Physics & Applied Math Engineering Technology ATTN: R. Helzer P.O. Box 3999 Seattle, WA 98124
1	Lockheed Missile & Space Co., Inc. ATTN: J. Philips (O-54-50) P.O. Box 3504 Sunnyvale, CA 94088	1	Science Aplications International ATTN: R. Parkinson 5150 El Camino Real, Suite B-31 Los Altos, CA 94022

Aberdeen Proving Ground

45   Dir, USARL
        ATTN: AMSRL-SL-I, D. F. Haskell
                AMSRL-SL-B, P. H. Deitz
                AMSRL-SL-BA, J. Walbert
                AMSRL-SL-BS, J. T. Klopcic
                AMSRL-SL-BV, J. H. Smith
                AMSRL-CI, W. H. Mermagen, Sr.
                AMSRL-CI-C, W. B. Sturek
                AMSRL-CI-S, A. Mark
                AMSRL-WT-TA,
                   W. Bruchey
                   G. Bulmash
                   J. Dehn
                   G. Filbey
                   H. Meyer
                AMSRL-WT-TC,
                   G. Silsby
                   R. Coates
                   K. Kimsey
                   D. Scheffler
                AMSRL-WT-TD,
                   K. Frank
                   S. Segletes
                   J. Walter
                AMSRL-WT-PB,
                   C. Nietubicz
                   E. M. Schmidt
                AMSRL-WT-PE, G. Gazonas
                AMSRL-WT-WA,
                   B. Moore
                   H. Rogers
                AMSRL-WT-WC, J. Rocchio
                AMSRL-WT-WD,
                   A. Prakash (12 cp)
                   D. Eccleshall
                   C. Hollandsworth
                   C. Hummer
                   A. Niiler
                   G. Thomson
                AMSRL-WT-WE, J. Temperley
                AMSRL-WT-WG, L. Puckett

27

INTENTIONALLY LEFT BLANK.

USER EVALUATION SHEET/CHANGE OF ADDRESS

This Laboratory undertakes a continuing effort to improve the quality of the reports it publishes. Your comments/answers to the items/questions below will aid us in our efforts.

1. ARL Report Number __ARL-TR-326_____ Date of Report __December 1993_____

2. Date Report Received _____

3. Does this report satisfy a need? (Comment on purpose, related project, or other area of interest for which the report will be used.) _____

_____

_____

4. Specifically, how is the report being used? (Information source, design data, procedure, source of ideas, etc.) _____

_____

_____

5. Has the information in this report led to any quantitative savings as far as man-hours or dollars saved, operating costs avoided, or efficiencies achieved, etc? If so, please elaborate. _____

_____

_____

6. General Comments. What do you think should be changed to improve future reports? (Indicate changes to organization, technical content, format, etc.) _____

_____

_____

_____

CURRENT
ADDRESS

Organization _____

Name _____

Street or P.O. Box No. _____

City, State, Zip Code _____

7. If indicating a Change of Address or Address Correction, please provide the Current or Correct address above and the Old or Incorrect address below.

OLD
ADDRESS

Organization _____

Name _____

Street or P.O. Box No. _____

City, State, Zip Code _____

(Remove this sheet, fold as indicated, tape closed, and mail.)
(DO NOT STAPLE)

BUSINESS REPLY MAIL FIRST CLASS PERMIT No 0001, APG, MD	NO POSTAGE NECESSARY IF MAILED IN THE UNITED STATES

Postage will be paid by addressee.

Director
U.S. Army Research Laboratory
ATTN: AMSRL-OP-CI-B (Tech Lib)
Aberdeen Proving Ground, MD 21005-5066